ULTRASONIC IMAGING 16, 164-175 (1994)

EFFICIENT TWO-DIMENSIONAL BLOCKED ELEMENT COMPENSATION

Pai-Chi Li and M. O'Donnell

Electrical Engineering and Computer Science Department
and Bioengineering Program
University of Michigan
Ann Arbor, MI 48109-2122

Very large, two-dimensional, anisotropic arrays have been proposed to improve ultrasound image quality. Due to noncontiguous acoustic windows into the body, however, a significant portion of such an aperture may be blocked. Blocked elements result in high sidelobes in the point spread function, degrading image quality. To compensate for this, an object dependent method using multiple receive beams has been recently proposed. This method is effective in removing undesired sidelobes. However, previous results were for one-dimensional arrays where only lateral beams were used for estimation. With two-dimensional arrays, the distribution of blocked elements can change beam characteristics, both laterally and elevationally. In other words, receive beams must be formed in both directions for better performance. Although straightforward in principle, extension of the algorithm from one dimension to two increases computational complexity dramatically. Furthermore, the restricted elevational steering capability of anisotropic arrays also limits performance. In this paper, several computationally efficient algorithms for two-dimensional blocked element compensation are proposed and evaluated. It is shown that undesired sidelobes can be effectively removed using only a limited number of receive beams. Image quality can therefore be restored in the presence of blocked elements without significantly increasing hardware complexity.

Key words: Anisotropic array; blocked element compensation; detectability; multiple receive beamforming; very large array.

1. INTRODUCTION

Current diagnostic ultrasonic imagers using one-dimensional arrays have not been successful in cancer diagnosis due to the inability to detect low contrast lesions deep in the body, such as tumors. To enhance low contrast detectability as well as present fine spatial detail, both spatial and contrast resolution must be improved. In other words, the size of the three-dimensional resolution volume must be reduced. To achieve this, various large, two-dimensional arrays have been investigated [1–5]. In particular, two-dimensional, anisotropic arrays (also known as 1.5 dimensional arrays) have been proposed to improve image quality [6–11]. These arrays are undersampled in the non-scan direction to reduce the total channel count. In addition, they can be used to correct for image artifacts due to noncontiguous acoustic windows and sound velocity inhomogeneities. They are not, however, suitable for real-time three-dimensional imaging due to the limited steering capability in elevation.

0161-7346/94 $6.00

Phase aberrations due to sound velocity inhomogeneities are likely to produce wavefront distortion disrupting diffraction patterns. Furthermore, if conformal array structures are used to maintain good contact with the body over a large area, array geometric irregularities can also produce catastrophic image degradation. To estimate large phase excursions across the array, a correlation based method has been proposed [12–14]. Recent progress in phase aberration correction associated with large, anisotropic, conformal arrays has also been reported in [5,15,16].

As shown in figure 1, a significant portion of the array may be blocked if the aperture is large. Blocked elements receiving either no signals or strong reverberations can be detected using the receive amplitude distribution across the array. Such elements should be turned off in order not to contribute to beamforming. Consequently, with a fully adaptive system, blocked elements can be translated into inoperable elements. Depending on their number and position, these inoperable elements are likely to produce severe artifacts. Generally, inoperable elements result in higher sidelobes deteriorating contrast resolution. Furthermore, spatial resolution is degraded if the total aperture size is reduced.

A blocked element compensation algorithm has been proposed for one-dimensional arrays [17]. Multiple receive beams in the lateral direction were used at each transmit angle and receive range in a sector scan image to measure local statistics and to estimate the lateral acoustic source distribution. Experimental results on point targets showed that beamforming artifacts can be dramatically reduced. Combined with local statistics, results on distributed targets also demonstrated that the modified algorithm can effectively enhance contrast resolution.

Factors affecting detectability in the presence of blocked elements were studied using area-wise speckle statistics [18]. Improvements with compensation were quantified using the contrast-to-noise ratio (CNR). It was shown that contrast resolution is determined mainly by both the number of independent speckles and sidelobe energy. If the total aperture size is not reduced, the number of independent speckles does not change and sidelobes dominate low contrast detectability. In the examples presented in [18], detectability can be fully recovered even with 25% of the elements inoperable. In most clinical situations, this method may play an essential role in fully realizing the potential of large array systems.

Previous results on blocked element compensation only considered lateral sidelobes. Undesired sidelobes in elevation cannot be estimated since one-dimensional arrays cannot steer in this direction. With two-dimensional arrays, blocked elements can also change the characteristics of elevational beam patterns. Therefore, scattering source profiles must be estimated in both azimuth and elevation and the blocked element compensation algorithm

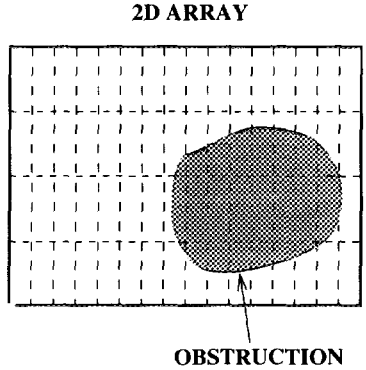

Fig. 1 Blocked array elements with two-dimensional anisotropic arrays.

must be extended from one dimension to two. Although straightforward in principle, one critical issue with anisotropic arrays is their ability to form multiple beams in elevation. Since the element size of anisotropic arrays in the non-scan direction can be as large as several wavelengths, grating lobes occur limiting elevational steering. Degradation due to grating lobes must be considered in designing compensation algorithms for two-dimensional arrays.

Two-dimensional blocked element compensation is computationally complex. Since one independent delay-and-sum structure is needed for one receive beam, direct extension of the one-dimensional algorithm to two dimensions squares the order of complexity. To simplify computations, three algorithms with reduced sets of multiple receive beams are investigated in this paper. Performance is also evaluated based on simulation results.

In the next section, the basic principles of two-dimensional blocked element compensation are presented. Efficient algorithms are proposed and explored in section 3. This paper concludes in section 4 with a discussion of the results.

2. BASIC PRINCIPLES OF TWO-DIMENSIONAL BLOCKED ELEMENT COMPENSATION

Degraded beam patterns due to blocked array elements can be modeled as a superposition of two patterns, one produced by the full aperture and the other by blocked elements with a negative driving signal. In general, higher sidelobe levels are observed in the corrupted beam pattern, degrading contrast resolution. In addition, if blocked elements are located at the array edge, i.e., if the total aperture size is reduced, a wider mainlobe results, degrading spatial resolution. The goal of blocked element compensation is to restore contrast resolution by removing undesired sidelobe contributions. Spatial resolution cannot be recovered, however, due to physical limitations.

Sidelobes in the point spread function produce undesired image artifacts. On transmit, sidelobes insonify objects outside of the desired focal spot creating undesired acoustic sources. On receive, these undesired sources contribute to the image point due to sidelobes of the receive beam pattern. As the number of blocked elements increases, undesired sidelobe contributions grow. Therefore, the starting point of blocked element compensation is to estimate at a given range and transmit angle both the acoustic source distribution (produced by the transmit beam) and the contributions of these sources at the image point (produced by the receive beam). Unfortunately, the actual source profile is unknown in practice. It can be estimated, however, using fixed direction transmit and all direction receive focusing (i.e., multiple receive beamforming).

Considering the lateral response with one-dimensional arrays, this problem can be formulated as follows. Define the lateral distribution of acoustic sources as

$$\mathbf{a} = [a(1), \cdots, a(m)]^T \quad , \tag{1}$$

where $a(i)$ is the complex weighting (i.e., strength and phase) of the i^{th} source. The measured lateral source profile after receive beamforming is

$$\mathbf{x} = [x(1), \cdots, x(n)]^T \quad , \tag{2}$$

where n is the number of discrete samples satisfying the spatial Nyquist criterion for the receive beam pattern over the entire scan plane. Assuming the number of sources is less than the number of independent beam directions ($m < n$), with the m sources

positioned at azimuthal angles $\Delta_1, \cdots, \Delta_m$ respectively, a matrix $\mathbf{B}$ of dimension $n \times m$ can be constructed where the i^{th} column in $\mathbf{B}$ is simply the lateral receive beam pattern centered at Δ_i. In other words,

$$\mathbf{B} \stackrel{def}{=} \begin{pmatrix} bp(\sin\theta_1 - \Delta_1) & bp(\sin\theta_1 - \Delta_2) & \cdots & bp(\sin\theta_1 - \Delta_m) \\ bp(\sin\theta_2 - \Delta_1) & bp(\sin\theta_2 - \Delta_2) & \cdots & bp(\sin\theta_2 - \Delta_m) \\ \vdots & \vdots & \vdots & \vdots \\ bp(\sin\theta_n - \Delta_1) & bp(\sin\theta_n - \Delta_2) & \cdots & bp(\sin\theta_n - \Delta_m) \end{pmatrix} , \tag{3}$$

where $\sin\theta_i$ is the direction of the i^{th} lateral beam line and $bp(\sin\theta)$ is the receive beam pattern evaluated at direction $\sin\theta$. The receive beam pattern at any range for a dynamically focused system can be approximated by a continuous wave model. In other words, it is obtained by Fourier transforming the real aperture function, where aperture weights are one for active elements and zero for inactive elements. Since the Fourier transform approximation is only valid in the limit of continuous wave excitation, model error exists in the matrix $\mathbf{B}$.

Given $\mathbf{B}$, the measured source profile can be modeled as the following convolution sum:

$$\mathbf{B}\ \mathbf{a} = \mathbf{x} \quad . \tag{4}$$

Using this model, the azimuthal angles and weighting of the complex sources (i.e., strength and time delay) can be estimated by solving the following minimization problem

$$\hat{\Delta}_i's, \hat{\mathbf{a}} = \min_{\Delta_i's, \mathbf{a}} ||\mathbf{B}\ \mathbf{a} - \mathbf{x}||_2 \quad , \tag{5}$$

where we use the l_2-norm to measure the error between the estimated profile ($\mathbf{Ba}$) and the measured source profile ($\mathbf{x}$). Note that Eq. (5) is a highly nonlinear problem. To solve it, directions of scattering sources (i.e., $\Delta_1, \cdots, \Delta_m$) are first estimated by peak finding. Hence, the minimization problem reduces to the following form:

$$\hat{\mathbf{a}} = \min_{\mathbf{a}} ||\mathbf{Ba} - \mathbf{x}||_2 \quad . \tag{6}$$

In Eq. (6), $\mathbf{B}$ represents an imperfect model where imperfections are due to both the continuous wave approximation for receive beam patterns and the assumption of delta functions for the scattering source distribution. Therefore, Eq. (6) should be solved using the Total-Least-Squares (TLS) method instead of standard Least-Squares (LS) methods. In other words, both model error (i.e., error in $\mathbf{B}$) and measurement error (i.e., error in $\mathbf{x}$) should be minimized. Details of the TLS method can be found in [19,20].

With two-dimensional arrays, the measured source profile ($\mathbf{x}$) can also be obtained in elevation. In this case, $\mathbf{a}$ represents the elevational scattering source distribution at a given range and transmit direction. Similarly, elevational beam patterns can be approximated by Fourier transforming the aperture functions.

The scattering source distribution can also be estimated using multiple lines of receive beams in both lateral and elevational directions. In other words, we have

$$\mathbf{a} = [\mathbf{a}_1^T|\mathbf{a}_2^T|\cdots|\mathbf{a}_N^T]^T \quad , \tag{7}$$

where $\mathbf{a}_i$ represents the distribution of m_i acoustic sources on a lateral or elevational line. Note that the number of acoustic scatterers on each line is generally independent of each other (i.e., $m_i \neq m_j$ if $i \neq j$). On the other hand, multiple lines of receive beams can be written as

$$\mathbf{x} = [\mathbf{x}_1^T|\mathbf{x}_2^T|\cdots|\mathbf{x}_N^T]^T \quad , \tag{8}$$

where $\mathbf{x}_i$ represents one line of lateral or elevational receive beams. The matrix $\mathbf{B}$ can be represented as

$$\mathbf{B} \stackrel{def}{=} \begin{pmatrix} \mathbf{B}_1 & \mathbf{0} & \cdots & \mathbf{0} \\ \mathbf{0} & \mathbf{B}_2 & \cdots & \mathbf{0} \\ \vdots & \vdots & \vdots & \vdots \\ \mathbf{0} & \mathbf{0} & \cdots & \mathbf{B}_N \end{pmatrix} \quad , \tag{9}$$

where $\mathbf{B}_i$ is the convolution operator for each receive beam line. Note that contributions from sources outside the beam line are ignored such that $\mathbf{B}$ has a block-diagonal form. Although these contributions can be included in the formulation, they considerably increase the number of computations.

The TLS solution, $\hat{\mathbf{a}}$, satisfies

$$\hat{\mathbf{B}}\hat{\mathbf{a}} \stackrel{def}{=} (\mathbf{B}+\mathbf{E})\hat{\mathbf{a}} = (\mathbf{x}+\mathbf{e}) \quad , \tag{10}$$

where $\mathbf{E}$ is the estimated model error, $\mathbf{e}$ is the estimated measurement error and the Frobenius norm of the matrix $[\mathbf{E}|\mathbf{e}]$ is the minimized total error. Each column in $\hat{\mathbf{B}}$ represents an independently corrected beam pattern centered at an acoustic source direction. With $\hat{\mathbf{B}}$ and $\hat{\mathbf{a}}$, undesired contributions from sidelobes of outside objects can be estimated and removed.

As mentioned in [17, 18], local statistics obtained from multiple receive beams can be used to determine if the TLS method is applicable. In other words, if the image point is in an anechoic region embedded in a speckle background, sidelobes from the background considerably increase its intensity and possibly create nonexisting acoustic sources in the TLS estimation. Hence, discriminating between different tissue types is necessary. A point-wise, acoustic signal-to-noise ratio (SNR), defined as the ratio of mean to standard deviation of the envelope of the scattered signal, is therefore used for this purpose. In general, a high SNR (higher than 2.5 in the examples shown in this paper) indicates the image point is in an anechoic region. Hence, in this algorithm, the acoustic SNR is first calculated using multiple receive beams. The TLS method is only applied if the SNR is lower than a prespecified threshold (i.e., 2.5).

For further details of the algorithm, please refer to [17, 18].

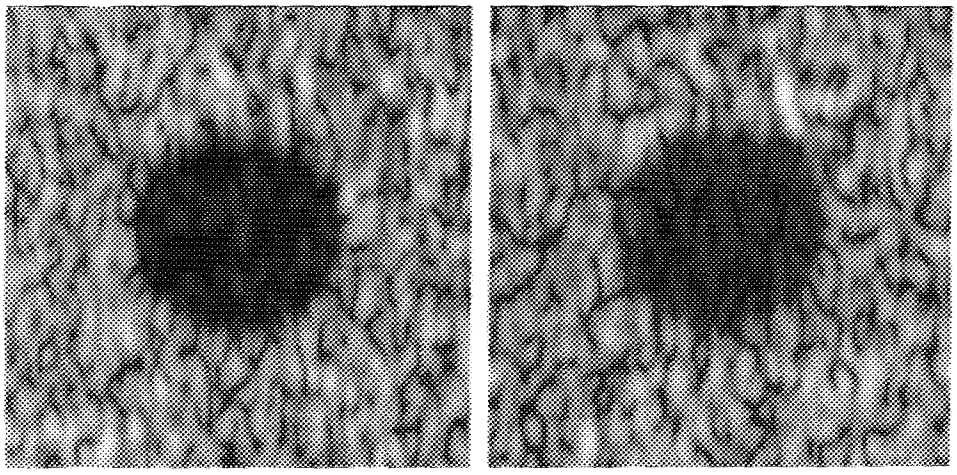

Fig. 2 Images of a spherical object with a two-dimensional array.

3. SIMULATION RESULTS

Simulations are performed to test the efficacy of several two-dimensional blocked element compensation algorithms. In all simulations, images of a spherical, anechoic region are made using a two-dimensional square array with 32 elements in the scan direction and 8 elements in elevation. In other words, the array element size in the non-scan direction is four times that in the scan direction. All images consist of a 128×128 grid, where the vertical axis represents the axial direction and the horizontal axis azimuth, i.e., simulated images are in a sector format prior to scan conversion. In this format, the point spread function is space invariant and separable. Note that 128 beams in the lateral direction represent a 90^o sector and 128 samples in the axial direction represent approximately a 10 mm distance at a 10 MHz sampling rate. All simulated objects in this paper are centered on the array normal and are spherical in the unconverted format. These objects are approximately elliptic in a two-dimensional sector scan format. The envelope of the axial response has a Gaussian shape with a 35% fractional bandwidth. The lateral and elevational responses, on the other hand, are simply obtained using a continuous wave model. Speckle patterns are simulated using the procedure described in [18].

Two images are shown in figure 2 over a 40 dB display range. The left panel has no blocked elements and the right panel has blocked elements (a cross segment extending over elements 4-12 in the scan direction and elements 5-7 in the non-scan direction). Clearly, undesired sidelobes from the background increase the brightness in the anechoic region, thus reducing contrast. To restore contrast resolution, sidelobes from the speckle background must be removed.

Figure 3 shows the first scheme (BEC_2D1) in which only beams along the lateral direction in the image plane are used, similar to the one-dimensional case. In other words, $\mathbf{B}$, $\mathbf{a}$ and $\mathbf{x}$ are exactly the same as described in Eqs. (1), (2) and (3). Positions of receive beams (i.e., $\mathbf{x}$) are also indicated in figure 3. Compensated images using this simplified scheme are shown in figure 4. In this figure, as well as the following two figures of simulated images, the left panel shows the compensated image with no blocked elements and the right panel shows the compensated image with the same blocked elements used for the right panel of figure 2. It is evident that the performance is

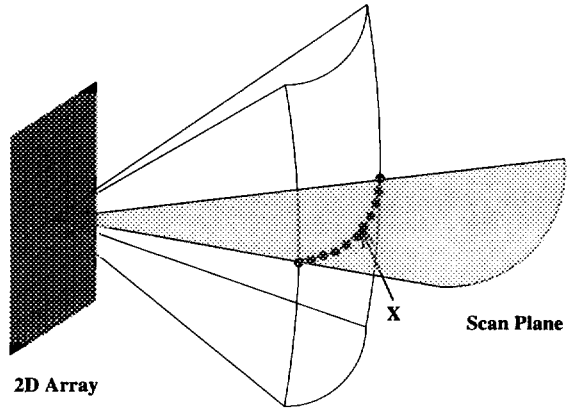

BEC_2D1

Fig. 3 A reduced set of multiple receive beams for blocked element compensation with two-dimensional arrays (BEC_2D1).

limited, although some undesired contributions are removed. The primary reason is that elevational contributions are difficult to estimate using only lateral beams.

The second scheme (BEC_2D2) is shown in figure 5. In this method, receive beams are formed only on principle axes (azimuth and elevation) and no off-axis beams are used.

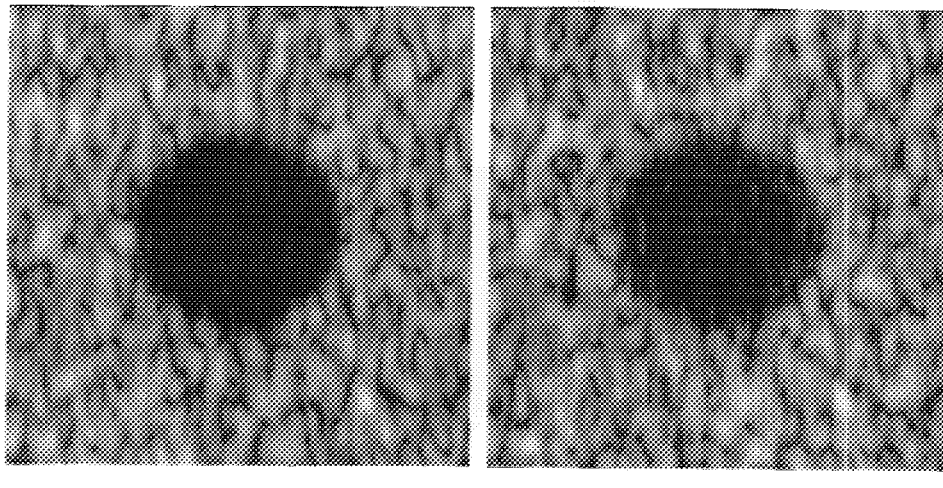

Fig. 4 Images with blocked element compensation (BEC_2D1).

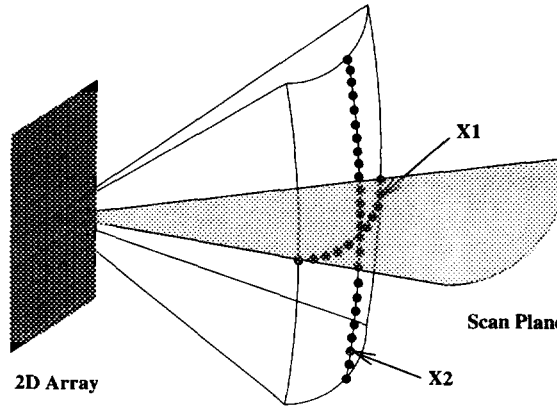

BEC_2D2

Fig. 5 A reduced set of multiple receive beams for blocked element compensation with two-dimensional arrays (BEC_2D2).

Therefore, we have

$$\mathbf{B} \stackrel{def}{=} \begin{pmatrix} \mathbf{B}_1 & \mathbf{0} \\ \mathbf{0} & \mathbf{B}_2 \end{pmatrix} , \tag{11}$$

$$\mathbf{a} = [\mathbf{a}_1^T | \mathbf{a}_2^T]^T \tag{12}$$

and

$$\mathbf{x} = [\mathbf{x}_1^T | \mathbf{x}_2^T]^T . \tag{13}$$

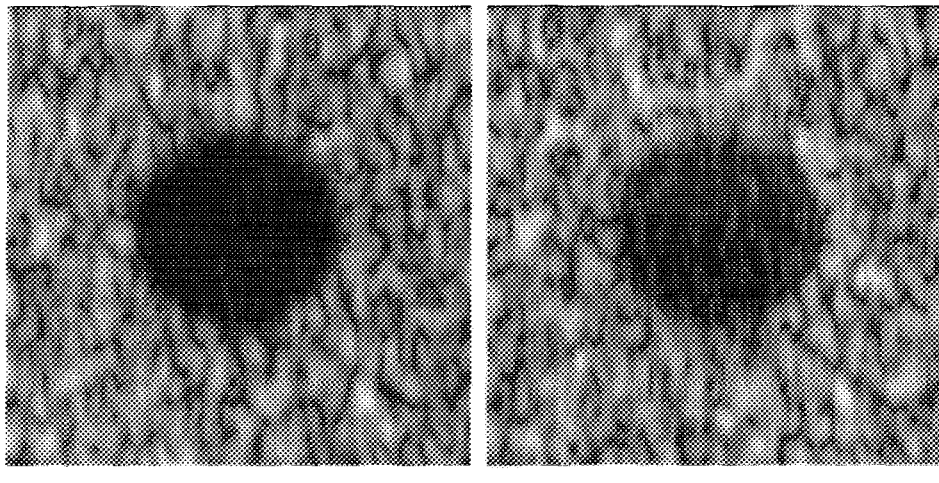

Fig. 6 Images with blocked element compensation (BEC_2D2).

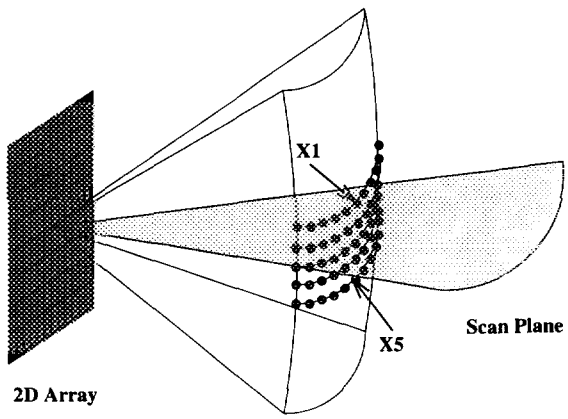

Fig. 7 A reduced set of multiple receive beams for blocked element compensation with two-dimensional arrays (BEC_2D3).

Positions of $\mathbf{x}_i$'s are also indicated in figure 5. The compensated images using this scheme are shown in figure 6 and indicate minimal improvement over the original image. Reduced quality compared to the simple one-dimensional correction of figure 3 is also clearly illustrated.

Finally, the third scheme (BEC_2D3) is shown in figure 7. In this method, receive beams are formed along five lateral lines near the image plane. The inclination between

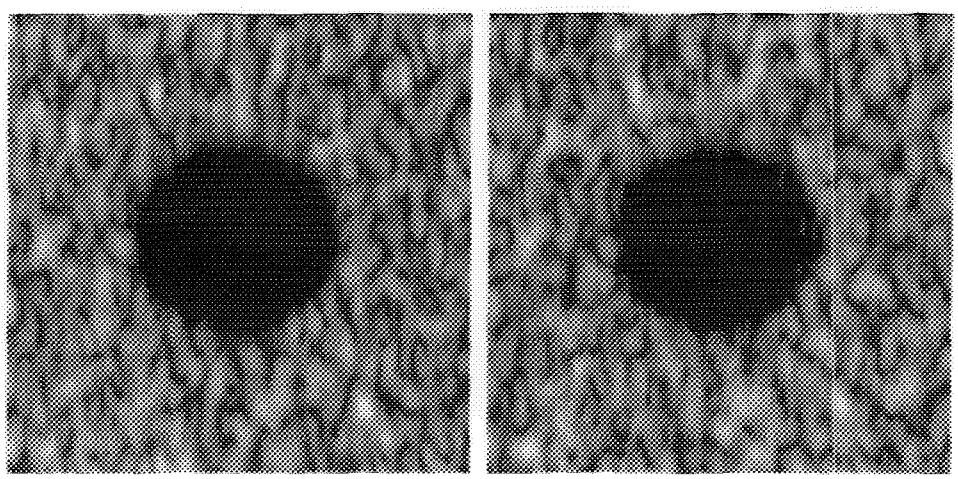

Fig. 8 Images with blocked element compensation (BEC_2D3).

two lateral lines is the spatial Nyquist interval. Therefore, we have

$$\mathbf{B} \stackrel{def}{=} \begin{pmatrix} \mathbf{B}_1 & \mathbf{0} & \cdots & \mathbf{0} \\ \mathbf{0} & \mathbf{B}_2 & \cdots & \mathbf{0} \\ \vdots & \vdots & \vdots & \vdots \\ \mathbf{0} & \mathbf{0} & \cdots & \mathbf{B}_5 \end{pmatrix} , \tag{14}$$

$$\mathbf{a} = [\mathbf{a}_1^T | \mathbf{a}_2^T | \cdots | \mathbf{a}_5^T]^T \tag{15}$$

and

$$\mathbf{x} = [\mathbf{x}_1^T | \mathbf{x}_2^T | \cdots | \mathbf{x}_5^T]^T \quad . \tag{16}$$

Positions of $\mathbf{x}_i$'s are indicated in figure 7 and compensated images are shown in figure 8. This method effectively reduces undesired contributions and performs the best of the three. Possible reasons are: first, near sidelobes are readily estimated. Second, statistical analysis is more robust given a larger number of receive beams.

4. DISCUSSION

The original one-dimensional blocked element compensation algorithm has been extended to two dimensions. To reduce hardware complexity and provide good performance, three computationally efficient schemes have been investigated. Although all schemes can reduce undesired sidelobes, performance depends on both the number and position of parallel receive beams used for estimation. Results showed that BEC_2D3 (Fig. 7) provides a good tradeoff between complexity and performance.

Grating lobes of two-dimensional, anisotropic arrays were not considered in the examples presented in this paper. With grating lobe effects, performance of BEC_2D1 (Fig. 3) and BEC_2D3 is expected not to change significantly since no elevational steer is required for BEC_2D1 and only small inclinations are used for BEC_2D3. The second scheme (i.e., BEC_2D2, Fig. 5), however, is expected to have worse performance since it requires receive beams across a large elevational span.

With distributed targets, local statistics measured from multiple receive beams are an essential component of the blocked element compensation algorithm. To obtain accurate estimation of local statistics, a larger number of receive beams is required. This is one reason why BEC_2D3 performs the best among all three methods.

Instead of delay-and-sum structures, an alternative method presented in [21] can be used for parallel receive beamforming. This method uses spatial Fourier processing to produce multiple simultaneous beams of high precision with little increase in the complexity of a fully digital beam former. It was shown that up to nine high quality simultaneous beams spaced at the spatial Nyquist interval can be produced by this method. Therefore, this method can be combined with BEC_2D3 to form multiple (five in this case) beams in elevation while reducing hardware required for parallel receive beamforming.

In spite of the limited elevational steering capability of two-dimensional, anisotropic arrays, BEC_2D3 demonstrates one example of using limited elevational steer to improve image quality. Other applications of two-dimensional, anisotropic arrays should be further explored.

ACKNOWLEDGMENTS

Support supplied by the National Institutes of Health under Grant CA 54896 and by the General Electric Company is gratefully acknowledged.

REFERENCES

[1] Sheikh, K.H., Smith, S.W., von Ramm, O.T. and Kisslo, J., Real-time, three-dimensional echocardiography: feasibility and initial use, *Echocardiography 8*, 199-225 (1991).

[2] Smith, S.W., Trahey, G.E. and von Ramm, O.T., Two-dimensional arrays for medical ultrasound, *Ultrasonic Imaging, 14*, 213-233 (1992).

[3] Turnbull, D.H., Kerr, A.T. and Foster, F.S., Simulation of B-scan Images from Two-dimensional Transducer Arrays, in *Proceedings of the 1990 IEEE Ultrasonics Symposium*, pp. 769-773, IEEE Cat. No. 90CH2938-9 (IEEE, New York, 1990).

[4] Turnbull, D.H. and Foster, F.S., Beam steering with pulsed two-dimensional transducer arrays, *IEEE Trans. Ultrason, Ferroelec., Freq. Contr. 38*, 320-333 (1991).

[5] O'Donnell, M. and Li, P.-C., Aberration Correction on a Two-dimensional Anisotropic Phased Array, in *Proceedings of the 1991 IEEE Ultrasonics Symposium*, pp. 1189-1193, IEEE Cat. No. 91CH3079-1 (IEEE, New York, 1991).

[6] Takeuchi, H., Masuzawa, H., Nakaya, C. and Ito, Y., Medical Ultrasonic Probe Using Electrostrictive Ceramics/Polymer Composite, in *Proceedings of the 1989 IEEE Ultrasonics Symposium*, pp. 705-708, IEEE Cat. No. 89CH2791-2 (IEEE, New York, 1989).

[7] Takeuchi, H., Masuzawa, H. and Nakaya, C., Relaxor Ferroelectric Transducers, in *Proceedings of the 1990 IEEE Ultrasonics Symposium*, pp. 697-705, IEEE Cat. No. 90CH2938-9 (IEEE, New York, 1990).

[8] Smith, L.S., Engeler, W.E., O'Donnell, M. and Piel, J.E., Jr., Rectilinear Phased Array Transducer Using 2-2 Ceramic-Polymer Composite, in *Proceedings of the 1990 IEEE Ultrasonics Symposium*, pp. 805-808, IEEE Cat. No. 90CH2938-9 (IEEE, New York, 1990).

[9] Daft, C.M.W., Smith, S. and O'Donnell, M., "Beam Profiles and Images from Two-Dimensional Arrays", in *Proceedings of the 1990 IEEE Ultrasonics Symposium*, pp. 775-779, IEEE Cat. No. 90CH2938-9 (IEEE, New York, 1990).

[10] Smith, W.A., "New Opportunities in Ultrasonic Transducers Emerging from Innovations in Piezoelectric Materials", in *SPIE 1733 New Developments in Ultrasonic Transducers and Transducer Systems*, pp. 3-26, (SPIE, Bellingham, 1992).

[11] Thomas, L., Wildes, D., Smith, L.S., Daft, C.M.W. and Rigby, W., Current Status and Future Prospects for High Channel Count Ultrasonic Imagers, *the 36th Annual Meeting and Exhibition of American Association of Physicists in Medicine*, (AAPM, Anaheim, 1994).

[12] Flax, S.W. and O'Donnell, M., Phase aberration correction using signals from point reflectors and diffuse scatterers: Basic principles, *IEEE Trans. Ultrason., Ferroelec. Freq. Contr. 35*, 758-767 (1988).

[13] O'Donnell, M. and Flax, S.W., Phase aberration correction using signals from point reflectors and diffuse scatterers: Measurement, *IEEE Trans. Ultrason., Ferroelec. Freq. Contr. 35*, 768-774 (1988).

[14] O'Donnell, M. and Flax, S.W., Phase aberration correction using signals from point reflectors and diffuse scatterers: Human studies, *Ultrasound Imaging, 10*, 1-11 (1988).

[15] O'Donnell, M. and Engeler, W.E., Correlation-based aberration correction in the presence of inoperable elements, *IEEE Trans. Ultrason., Ferroelec. Freq. Contr. 39*, 700-707 (1992).

[16] Li, P.-C. and O'Donnell, M., Phase aberration correction on two-dimensional conformal arrays, *accepted for publication in IEEE Trans. Ultrason., Ferroelec. Freq. Contr.*, (1993).

[17] Li, P.-C., Flax, S.W., Ebbini, E.S. and O'Donnell, M., Blocked element compensation in phased array imaging, *IEEE Trans. Ultrason., Ferroelec. Freq. Contr. 40*, 283-292 (1993).

[18] Li, P.-C. and O'Donnell, M., Improved detectability with blocked element compensation, *accepted for publication in Ultrasonic Imaging (1994)*.

[19] Golub, G.H. and Van Loan, C.F., An analysis of the total least squares problem, *SIAM J. Numer. Anal., 17*, 883-893 (1980).

[20] Van Huffel, S. and Vandewalle, J., *The Total Least Squares Problem: Computational Aspects and Analysis* (SIAM, Philadelphia, 1991).

[21] O'Donnell, M., Efficient Parallel Receive Beam Forming for Phased Array Imaging Using Phase Rotation", in *Proceedings of the 1990 IEEE Ultrasonics Symposium*, pp. 1495-1498, IEEE Cat. No. 90CH2938-9 (IEEE, New York, 1990).